

SUPERCONDUCTING LINAC FOR THE RISF

H. J. Kim, H. J. Cha, M. O. Hyun, H. J. Jang, D.-O Jeon, J. D. Joo, M. J. Joung, H. C. Jung, Y. C. Jung, Y. K. Kim, M. K. Lee, G.-T. Park, IBS, Daejeon, Korea

Abstract

The RISF (Rare Isotope Science Project) has been proposed as a multi-purpose accelerator facility for providing beams of exotic rare isotopes of various energies. It can deliver ions from proton to Uranium. Proton and Uranium beams are accelerated upto 600 MeV and 200 MeV/u respectively. The facility consists of three superconducting linacs of which superconducting cavities are independently phased. Requirement of the linac design is especially high for acceleration of multiple charge beams. In this paper, we present the RISF linac design, the superconducting cavity, and cryomodule.

INTRODUCTION

The RISF (Rare Isotope Science Project) accelerator has been planned to study heavy ion of nuclear, material and medical science at the Institute for Basic Science (IBS). It can deliver ions from proton to Uranium with a final beam energy, for an example, 200 MeV/u for Uranium and 600 MeV for proton, and with a beam current range from 8.3 pμA (Uranium) to 660 pμA (proton) [1, 2]. The facility consists of three superconducting linacs of which superconducting cavities are independently phased and operating at three different frequencies, namely 81.25, 162.5 and 325 MHz.

SUPERCONDUCTING LINAC

Lattice Design

The configuration of the RAON accelerator facility within the rare isotope science project (RISF) is shown in Fig. 1. An injector system accelerates a heavy ion beam to 500 keV/u and creates the desired bunch structure for injection into the superconducting linac. The injector system comprises an electron cyclotron resonance ion source, a low energy beam transport, a radio frequency quadrupole, and a medium energy beam transport. The superconducting driver linac accelerates the beam to 200 MeV/u. The driver linac is divided into three different sections as shown in Fig. 2: low energy superconducting linac (SCL1), charge stripper section (CSS) and high energy superconducting linac (SCL2). The SCL1 accelerates beam to 18.5 MeV/u. The SCL1 uses the two different families of superconducting resonators, i.e., quarter wave resonator (QWR) and half wave resonator (HWR). The CSS accepts beam at 18.5 MeV/u. The charge stripper strips electrons from heavy ion beams to enhance the acceleration efficiency in the high energy linac section. The SCL2 accepts beam at 18.5 MeV/u and accelerates it to 200 MeV/u. The SCL2 uses the two types of single spoke resonators, i.e., SSR1 and SSR2. The

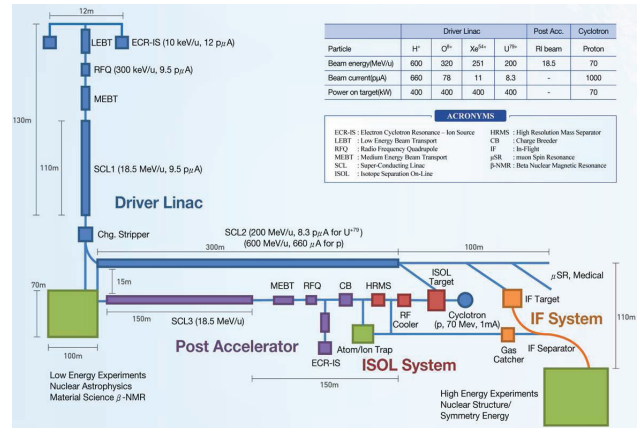


Figure 1: Layout of the RISF accelerator.

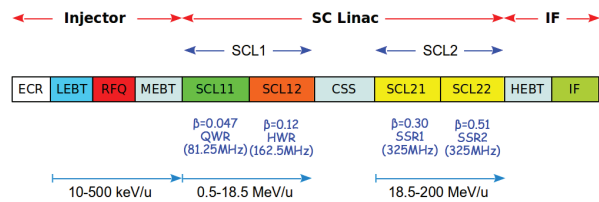


Figure 2: The RAON linear accelerator.

SCL2 provides beam into the in-flight fragmentation (IF) system via a high energy beam transport (HEBT).

The cavity optimum beta and frequency are chosen to maximize acceleration efficiency for each accelerating cavity and to minimize the beam loss. Quarter wave resonator segment is minimally used because of the dipole kick and the asymmetric field of quarter wave resonator. Unlike the quarter wave resonator, half wave resonator does not have the β -dependent dipole kick due to their symmetric nature of electromagnetic fields of the cavity. By adopting the half wave resonator, beam quality control becomes easier especially for high intensity beam operation. Single spoke resonators are applied in the high energy section after the charge stripper section because of the advantage that the single spoke resonator can have a larger bore radius. This is an advantage in reducing the uncontrolled beam loss in the high energy segment of the superconducting linac for high intensity operations. Optimization of the geometric betas of superconducting cavities is done and an optimum set of $\beta_g = [0.047, 0.12, 0.30, 0.51]$ is obtained. The parameters and requirement for the superconducting driver linac are given in Table 1.

The post accelerator (SCL3) is designed to accelerate the rare isotopes produced in the ISOL (Isotope Separation On-Line) system. The SCL3 is, in principle, a duplicate of the

Table 1: Parameters of the RAON superconducting linac for uranium and proton.

Parameters	unit	Requirement	
		Uranium	Proton
Beam species		Uranium	Proton
Input energy	MeV/u	0.5	0.5
Output energy	MeV/u	200	600
Beam power	kW	400	400
Horizontal emittance ($\epsilon_{x,r.m.s}$)	mm-mrad	0.19	0.14
Vertical emittance ($\epsilon_{y,r.m.s}$)	mm-mrad	0.17	0.12
Longitudinal emittance ($\epsilon_{z,r.m.s}$)	keV/u-ns	4.11	0.15
Bunch length	ps	20.5	8.5

Table 2: Machine Imperfection of RISP Lattice

Parameters	SC Cavity	Quadrupole
Displacement (mm)	± 1	± 0.15
Phase (deg)	± 1	-
Amplitude (%)	± 1	-
Rotation (mrad)	± 5	± 5

driver linac up to low energy linear accelerator. The accelerated rare isotope beams are reaccelerated in the SCL2. Hence, the RISP accelerator provides a large number of rare isotopes with high intensity and with various beam energies.

The linac lattice is optimized by minimizing emittance growth and potential for beam loss by keeping a beam envelope smooth and regular. A transverse phase advance per period is kept under 90 degrees to prevent envelope instabilities. The ratio of transverse to longitudinal phase advance is kept in the range of 1.2 to 1.6 to avoid a resonance due to parametric coupling between longitudinal and transverse planes.

For the actual SCL, machine imperfections cannot be avoided. The error comes from the misalignment of the linac elements and the limitation of manufacturing accuracy and various control errors. For instance, steering magnets are used to correct beam orbit displacements. In the baseline design of the RISP linac, steering magnets are placed where normal conducting quadrupoles are. The misalignment analysis includes all superconducting cavities and focusing elements assuming a uniform distribution.

Table 2 summarizes tolerances for the lattice consisting of superconducting cavity and normal conducting quadrupole. In the misalignment and RF error analysis, charge states of 33+ and 34+ of Uranium beams are used. Effect of machine imperfection on beam envelope is shown in Fig. 3. The maximum envelope is kept well below the transverse aperture 20 mm in the low energy linac. The envelope is under 25 mm in the high energy linac.

Superconducting Cavity

In the optimization of superconducting cavity, the fabrication cost, symmetry of transversal field around drift tubes, and minimization of peak fields are mainly con-

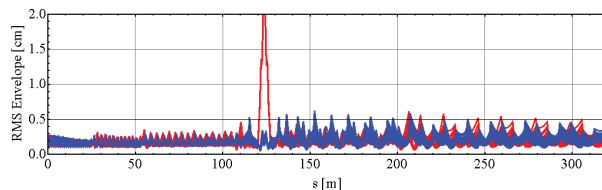


Figure 3: Plot of rms and maximum horizontal envelope for the driver linac due to machine imperfections.

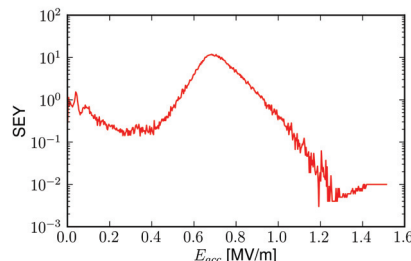


Figure 4: Plot of multipactor in QWR when Niobium is baked at 300°C.

cerned. The multipacting barriers of QWR are predicted by using CST PIC [3] code with the secondary emission yield (SEY) of a 300°C baked Niobium as shown in Fig. 4. Several peaks are shown in the plot of multipacting factors of 4 RF periods. The most serious multipactor occurs around the upper end of QWR at 1/8 of the accelerating gradient. The detuning due to the tolerances of fabrication and the frequency sensitivities to mechanical deforming are estimated. The cavity is fabricated by electron beam welding of hydroformed 3 mm Niobium sheets, drift tube and 4 additional ports without bottom flange. Two ports in the lower end are added for RF power and pickup coupling. The other two ports are installed for evacuation and high pressure rinsing. The predicted detunings and sensitivities of the bare cavity are shown in the Table 3.

SSR1 design has been upgraded. The previous design of SSR1 was based on end-walls with flat areas. In a recent design, the end-walls are changed from flat to round shape, as shown in Fig. 5. We have performed simulations on electromagnetic analysis with changing the design param-

Table 3: Detuning and Frequency sensitivities of QWR cavity.

Frequency shift	Value
Cavity length(upper)	-67kHz/mm
Cavity length(lower)	+1.3kHz/mm
Chemical etching(nose)	+20kHz/mm
Chemical etching(others)	-8.6kHz/mm
External pressure	-4.6Hz/mbar
Cool down(293K to 2K)	+200kHz
Lorentz force	-1.7Hz/(MV/m) ²

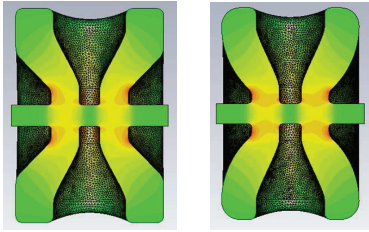


Figure 5: Design change of SSR1: flat end-walls (left) and round end-walls (right).

Table 4: Superconducting Cavity Parameters

Parameter	Unit	QWR	HWR	SSR1	SSR2
Frequency	MHz	81.25	162.5	325	325
β_g		0.047	0.12	0.30	0.51
$L_{eff} = \beta_g \lambda$	m	0.173	0.221	0.277	0.452
Q	10^9	2.1	4.1	9.2	10.5
QR_s	Ω	21	42	98	112
R/Q	Ω	468	310	246	296
E_{acc}	MV/m	5.2	5.9	6.9	8.6
E_{peak}/E_{acc}		5.6	5.0	6.3	7.2
B_{peak}/E_{acc}	mT/(MV/m)	9.3	8.2	6.63	7.2

eters of the single spoke resonator. It is not possible to design the cavity with simultaneously optimizing the figure-of-merit characteristics. Therefore, we determined the design parameters sensitive to the resonant frequency. The peak electric and magnetic fields were selected for minimizing the field emission in the cavity surface and maintaining the superconducting properties. Finally, the remaining design parameters were determined to maximize the R/Q and V_{acc} . Table 4 summarizes the parameters of four different superconducting cavities for the RISP superconducting linac.

Cryomodule

The linac has five types of cryomodules for four different kinds of cavities. The main roles of the cryomodules are maintaining operating condition of superconducting cavities and alignment of the cavities along the beam line. High level of vacuum and thermal insulation are required for the cryomodule to maintain the operating temperature of superconducting cavities. The cryomodules including QWR and HWR cavities are box-type while those including SSR1 and SSR2 cavities are cylindrical. The QWR is vertically installed while the HWRs are horizontally installed in the cryomodule as shown in Fig. 6. The main components of the cryomodule are dressed cavities and two phase pipe, power couplers to supply RF power to the cavities, tuners to control the operation of the cavities, and support systems to fix the cavities along the beam line. Since the operating temperature of the superconducting cavities are 2 K, 70 K thermal shield which is cooled by cold helium gas and 70 K and 4.5 K thermal intercepts are installed to minimize the thermal load. The cold mass including cavity string, cou-

Table 5: Thermal Load of Superconducting Linacs

	SCL11	SC12	SCL21	SCL22	SCL31	SCL33
Dynamic (W)	128.7	528.3	536.6	929.3	128.7	528.3
Static (W)	128.7	782.7	869.4	3780.0	128.7	782.7
Sum (W)	257.4	1311.0	1406.0	4709.3	257.4	1311.0

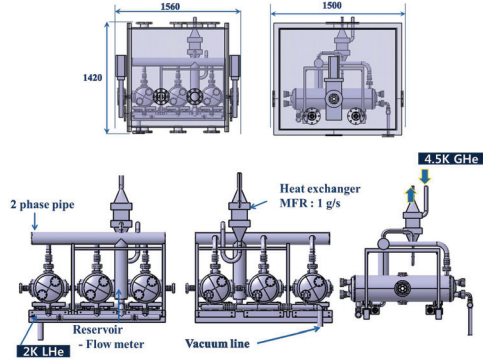


Figure 6: Layouts of HWR cryomodule.

pler and tuner is installed on the strong-back and then inserted into the vacuum vessel with thermal shield and MLI. The thermal load of superconducting linacs are summarized in Table 5. Dynamic and static loads are 70% and 30% out of the total thermal load, respectively. The design of the cryomodule components has been conducted based on the thermal and structural concerns. The thermal design starts from the estimation of the thermal loads that determine the required size of the components such as two phase pipes and other cryogenic pipes. Three levels of cryogenic flow are necessary such as 2 K, 4.5 K and 70K.

SUMMARY

The RISP linacs have been presented. In the design, four cavities, such as QWR, HWR, SSR1 and SSR2, are used to accelerate the beam in the linac. The parameters of the cavities are optimized. The box-shaped and cylindrical cryomodules are designed for hosting cavities.

ACKNOWLEDGMENTS

This work was supported by the Rare Isotope Science Project which is funded by the Ministry of Science, ICT and Future Planning (MSIP) and the National Research Foundation (NRF) of the Republic of Korea under Contract 2011-0032011.

REFERENCES

- [1] S.K. Kim et al, "Rare Isotope Science Project: Baseline Design Summary", <http://www.risp.re.kr/>
- [2] S.K. Kim et al, "RISP Workshop on Accelerator Systems", <http://indico.risp.re.kr/indico/conferenceDisplay.py?confId=2>
- [3] Computer Simulation Technology (CST), "CST Design Studio", <http://www.cst.com>